Radio Science, Volume 33, Number 4, Pages 803–819, July–August 1998

An analysis of leaky-wave dispersion phenomena in the vicinity of cutoff using complex frequency plane singularities

George W. Hanson and Alexander B. Yakovlev[1]
Department of Electrical Engineering and Computer Science, University of Wisconsin-Milwaukee

Abstract. In this paper we analyze characteristics of the dispersion function for leaky-wave modes in the vicinity of cutoff for several representative waveguiding structures. Our principal purpose is to demonstrate that in the vicinity of leaky-wave cutoff in open-boundary waveguides (in the spectral-gap region), dispersion behavior is controlled by the presence of branch points in the complex frequency plane. A similar situation occurs for the ordinary modes of homogeneously filled, perfefctly conducting cylindrical waveguides. These closed waveguides admit to simple analysis, leading to an explicit dispersion function which indicates frequency domain branch points. For open-boundary waveguides, the presence of frequency domain branch points is obscured by the necessity of numerically solving an implicit dispersion equation. A set of sufficient conditions is provided here which defines these branch points in a unified manner for both open and closed waveguides. Identification of these points allows for rapid determination of important and interesting regions in both the frequency and wavenumber planes and leads to increased understanding of dispersion behavior, especially in the case of dielectric loss. Examples are shown for several waveguiding geometries to demonstrate the general nature of the presented formulation.

1. Introduction

Leaky waves on open-boundary waveguides have been of interest for a long time [*Marcuvitz*, 1956; *Tamir and Oliner*, 1963], from both a theoretical and practical standpoint. The main utility of using leaky waves is to provide a concise and compact form, in restricted spatial regions, for the fields produced by a source in the presence of a waveguide that admits leaky-wave solutions. Leaky modes are usually implicated in a steepest-descent representation for the relevant integrals of a source-excited open-boundary waveguide. The literature in this area is extensive; several representative publications are by *Blok et al.* [1984], *Barkeshli et al.* [1990], *Jackson and Oliner* [1988], and *Collin* [1991].

Other than steepest-descent representations, leaky-mode expansions are described by *Carpentier and dos Santos* [1985, 1984] and *Tesler and*

[1]Also at North Carolina State University, Center for Advanced Computing and Communication, Raleigh, North Carolina

Copyright 1998 by the American Geophysical Union.

Paper number 98RS01440.
0048-6604/98/98RS-01440$11.00

Eichmann [1978], among others. A particularly relevant formulation is provided in a series of papers by *Haddon* [1986, 1987a, b, 1989], which served as the motivation for this work. Haddon's technique concerns transient elastic-wave phenomena, yet the relevant implicit dispersion relation is similar to those encountered in electromagnetic wave problems. Using this formulation, the transient elastic wave is computed over a deformed contour in the frequency plane, with the spatial inversion computed using proper and improper modes. The continuous radiation-mode component (branch cut integral in the transverse transform plane) is completely eliminated using this method. *Duffy* [1994] later implemented this method for electromagnetic transverse electric (TE) line source excitation of a grounded dielectric slab. In the above mentioned set of papers, identification of frequency domain branch points was crucial for implementation of the method.

Another related area that has received considerable attention lately is the topic of leaky waves supported by printed transmission lines [*Oliner*, 1987a; *Shigesawa et al.*, 1988, 1991, 1995; *Bagby et al.*, 1993; *Nghiem et al.*, 1996]. Open printed transmission line structures support space-wave leaky modes, which are used in antenna applications [*Oliner*, 1987b]. Currently, there is much interest in surface-wave leaky modes, which can lead to undesirable coupling, cross talk, and energy loss in a printed transmission line system. It has been found that the onset of surface-wave leakage (or leaky-wave cutoff) occurs in the spectral-gap region and that dispersion behavior in the spectral-gap region is significantly altered by the presence of dielectric loss [*Shigesawa et al.*, 1993]. This leaky-wave cutoff point (splitting point in the spectral-gap region, where several dispersion curves join together) for a lossless structure is identified as a fold point by *Yakovlev and Hanson* [1997], wherein a set of defining conditions which describe this point is presented. Qualitative normal forms which describe the dispersion behavior in the spectral-gap region are also presented.

In this paper, some frequency-plane singularities of the dispersion function for several guided-wave structures are examined. Motivated by symmetry conditions, it is shown that the previously mentioned fold point also identifies a frequency-plane branch point, residing on the real-frequency axis for lossless structures, at which frequency various branches of the dispersion function join together. Another type of branch point is also suggested by symmetry, leading to branch points in the complex frequency plane. This second type of branch point also satisfies the general conditions for the fold point, and so it is seen that the general fold point conditions are sufficient for both types of branch points. Theoretical and numerical results will be presented for several waveguiding structures.

2. Formulation

Consider a two-dimensional waveguiding structure, invariant along the waveguiding direction, taken here to be the z axis. The waveguiding media will be assumed isotropic, although the following results will apply to more general classes of media. In order to study the discrete modes which can be supported by the structure, Maxwell's equations are Fourier transformed temporally ($t \leftrightarrow \omega$) and along the waveguiding axis ($z \leftrightarrow \kappa$). The transformed equations are combined to form a homogeneous set of Helmholtz equations, which are then solved subject to appropriate boundary conditions. Equivalently, although with a change in interpretation, solutions of the same boundary value problem can be sought for a prescribed $e^{j(\omega t - \kappa z)}$ dependence. Either method yields an equation to determine the characteristic spectrum of discrete modes that the waveguide is capable of supporting, written here as

$$H(\kappa, \omega) = 0 \,. \tag{1}$$

It will be assumed here that $H : C^2 \to C$ is a smooth analytic function of the two complex variables (κ, ω). The dispersion function for discrete modes is obtained as the solution of (1),

generally in the form $\kappa_m(\omega)$, $m = 1, 2, 3, \ldots$. It is generally impossible to determine the dispersion function analytically, excepting a few simple cases, for example, a homogeneously filled, perfectly conducting cylindrical waveguide. It is shown in the following that certain symmetries in equation (1) lead naturally to the occurrence of frequency domain branch points of the dispersion spectrum $\kappa_m(\omega)$.

The considered class of problems will be planarly layered geometries of infinite extent, open or closed vertically, with or without perfectly conducting, infinitely thin strips. This class includes multilayered slab waveguides and multilayered, multiconductor printed transmission line geometries, among others. Examination of the implicit dispersion equation (1) for such structures leads to two observations. The first observation is that if κ is a root of the eigenvalue equation (1), $-\kappa$ is also a root of the same equation:

$$H(\kappa,\omega) = H(-\kappa,\omega) = 0\,. \tag{2}$$

It is clear that this condition will hold for any waveguiding structure, invariant along the waveguiding axis, composed of reciprocal media.

The second observation is that for real-valued material parameters (lossless media) and ω=Re$\{\omega\}$ or ω=Im$\{\omega\}$, if κ is a root of the eigenvalue equation (1), $\pm\kappa^*$ are also roots of the same equation:

$$\begin{aligned} H(\kappa,\omega) = H(\kappa^*,\omega) = 0 \\ H(-\kappa,\omega) = H(-\kappa^*,\omega) = 0 \end{aligned} \tag{3}$$

where $\pm\kappa^*$ are complex conjugates of $\pm\kappa$. The fact that complex roots occur in conjugate pairs is well known for shielded structures and can be observed for the considered class of problems by examination of the characteristic function H. The proof of (3) for the specific case of multilayered slab waveguides is the subject of *Tamir* [1967]. It is clear that if the branches $(\kappa, -\kappa)$ and (κ, κ^*) meet in the complex κ plane for some complex ω, that value of ω may represent a branch point which separates various branches of the dispersion function. The idea is to identify the frequencies ω for which branches $(\kappa, -\kappa)$ join together, and similarly for (κ, κ^*), and to provide conditions under which those frequencies are branch points of the dispersion function.

Accordingly, consider a point in the frequency plane $\omega = \omega_0$ at which $(\kappa, -\kappa)$ solutions of (1) become equal, i.e., $\kappa(\omega_0) = -\kappa(\omega_0) = 0$. Assuming that $(\kappa, -\kappa)$ are first-order zeros of (1) and become a second-order zero at ω_0 prompts the condition

$$H(0,\omega_0) = H'_\kappa(0,\omega_0) = 0\,. \tag{4}$$

Since we have two equations for the one complex variable, it suffices to determine ω_0 by solution of $H(0,\omega_0) = 0$.

Considering a point $\omega = \omega_1$ at which (κ, κ^*) solutions of (1) become equal, which again represents the coalescing of two first-order zeros of (1) to a second-order zero, leads to

$$H(\kappa_1,\omega_1) = H'_\kappa(\kappa_1,\omega_1) = 0\,. \tag{5}$$

While (4) and (5) define second-order zeros of H, these points are not necessarily branch points. Considering the point (κ_f, ω_f) to represent either $(0,\omega_0)$ or (κ_1,ω_1) for (4) and (5), respectively, it is found that the nonzero condition

$$\delta = H'_\omega(\kappa_f,\omega_f)H''_{\kappa\kappa}(\kappa_f,\omega_f) \neq 0 \tag{6}$$

is sufficient to guarantee ω_f is a branch point. In the following we will consider the branch point which separates $(-\kappa, \kappa)$ branches to be of ω_0 type and those which separate (κ, κ^*) (or their analytic continuation) to be of ω_1 type.

It should be noted that equations (5) and (6), which define the branch point ω_f in the ω plane, are the same as the definition of the fold point [*Golubitsky and Schaeffer*, 1985; *Seydel*, 1994] found in the (κ,ω) plane. The occurrence of a fold point in the spectral-gap region for conductor-backed coplanar strips has been discussed by *Yakovlev and Hanson* [1997]. It should be noted that in the event of material loss, complex conjugate solutions no longer exist, but two complex modes (those which become conjugate

modes when loss is removed) still coalesce at a complex fold point, given by (5) and (6). In the following, no notational difference will be made between the lossy and lossless cases.

To show that the fold point with coordinates (κ_f,ω_f) in the (κ,ω) plane determines a branch point ω_f in the ω plane, a Taylor series expansion in the vicinity of (κ_f,ω_f) can be applied. However, it necessitates a truncation of higher-order terms in the expansion, resulting in an approximation of the obtained results. Another way of showing the connection between the fold point and the branch point utilizes the normal form for the fold point obtained in the local neighborhood, as defined in [*Golubitsky and Schaeffer*, 1985; *Seydel*, 1994; *Yakovlev and Hanson*, 1997]

$$\begin{aligned}(\kappa-\kappa_f)^2+(\omega-\omega_f) \qquad & \delta>0\,,\\ (\kappa-\kappa_f)^2-(\omega-\omega_f) \qquad & \delta<0\end{aligned} \tag{7}$$

such that the normal form (equation (7)) qualitatively represents the dispersion function $H(\kappa,\omega)$ near (κ_f,ω_f).

Consider the case when $\delta>0$, resulting in the following representations for $\kappa(\omega)$:

$$\kappa(\omega)=\kappa_f\pm\sqrt{\omega_f-\omega} \qquad \omega<\omega_f\,, \tag{8}$$

$$\kappa(\omega)=\kappa_f\pm\jmath\sqrt{\omega-\omega_f} \qquad \omega>\omega_f\,. \tag{9}$$

Equation (8) represents a real-valued parabola equation, $Im\{\kappa(\omega)\}=0$. Equation (9) is equivalent to the form

$$Re\{\kappa(\omega)\}=\kappa_f\,, \qquad Im\{\kappa(\omega)\}=\pm\sqrt{\omega-\omega_f}$$

which defines a straight-line equation for $Re\{\kappa(\omega)\}$ and a parabola equation for $Im\{\kappa(\omega)\}$.

Since locally,

$$\kappa(\omega)=\kappa_f\pm\sqrt{-(\omega-\omega_f)}$$

it would seem to identify branch points at $\omega=\omega_f$ which cause branches of the κ function to meet. It should be noted that $\kappa_f=0$ indicates the branch point $\omega=\omega_f=\omega_0$ separating $(\kappa,-\kappa)$, and $\kappa_f\neq 0$ indicates the branch point $\omega=\omega_f=\omega_1$ separating (κ,κ^*).

The above analysis is correct assuming that the fold point (κ_f,ω_f) is real valued, such that the normal form (equation (7)) is applied only for real valued δ. A more general proof for complex (κ_1,ω_1) follows from the Weierstrass preparation theorem [*Bochner and Martin*, 1948].

Following the Weierstrass preparation theorem, let $H(\tilde{z},z_n)$ with the notation $\tilde{z}=(z_1,...,z_{n-1})$ be holomorphic (analytic) in a neighborhood of the origin $0\in\mathbf{C}^n$, with

$$H(0,0)=0\,, \qquad H(0,z_n)\neq 0\,.$$

The origin $0\in\mathbf{C}^n$ is used for convenience; any point can be translated to the origin by a smooth linear change of variables. Then there exists a neighborhood Ω of the origin and a function $U(\tilde{z},z_n)$ which is analytic and nonvanishing in Ω such that throughout Ω, H can be factored in the form

$$\begin{aligned}H(\tilde{z},z_n)=(z_n^p+a_{p-1}(\tilde{z})z_n^{p-1}+\cdots+\\ +a_1(\tilde{z})z_n+a_0(\tilde{z}))U(\tilde{z},z_n)\end{aligned} \tag{10}$$

where the a_j are holomorphic functions in a neighborhood of $0\in\mathbf{C}^{p-1}$ and $a_j(0)=0$ for $j=0,...,p-1$. If the integer p is taken to be the order of the zero of $H(0,z_n)$ at $z_n=0$, then the functions U, a_j, $j=0,...,p-1$ are uniquely determined.

Therefore the Weierstrass preparation theorem states that the holomorphic function H of two complex variables (ω,κ) in a neighborhood of $(\omega_f,\kappa_f)=(0,0)$ can be factored in the form

$$H(\omega,\kappa)=U(\omega,\kappa)\times W(\omega,\kappa) \tag{11}$$

where $U(\omega,\kappa)$ is a holomorphic function, $U(0,0)\neq 0$, and

$$W(\omega,\kappa)=\kappa^2+a_1(\omega)\kappa+a_0(\omega) \tag{12}$$

is a Weierstrass polynomial of order 2, wherein κ and ω are interchanged from (1) for convenience. The characteristic equation (1) in a neighborhood of $(0,0)$ is equivalent to a quadratic equation in κ

$$\kappa^2 + a_1(\omega)\kappa + a_0(\omega) = 0 . \quad (13)$$

It can be seen that $H(0,0) = 0$ is equivalent to $a_0(0) = 0$ and $H'_\kappa(0,0) = 0$ is equivalent to $a_1(0) = 0$. The solution of the quadratic equation (13) is given as

$$\kappa(\omega) = -\frac{a_1(\omega)}{2} \pm \frac{\sqrt{a_1^2(\omega) - 4a_0(\omega)}}{2} . \quad (14)$$

Let $d(\omega) = (2\kappa + a_1)$ and $c(\omega) = (a_1^2 - 4a_0)$ such that $d^2 = c$ with c analytic and $c(0) = 0$. If $c'(0) \neq 0$, then there is no analytic function d such that $d^2 = c$. To prove the last statement, assume d is analytic and take the derivative of $d^2 = c$ to get $2dd' = c'$. Since the left side of the last expression is zero ($d(0) = 0$), the right side must be zero, leading to a contradiction. Hence if $c'(0) \neq 0$, then d is nonanalytic, showing that κ is nonanalytic. It is easy to see that $c' \neq 0$ leads to $a'_0 \neq 0$, which in turn is equivalent to $H'_\omega \neq 0$ by (11) and (12). The nonanalytic point is easily seen to be a branch point due to the multivalued nature of (14), where a_1, a_0 can be expanded in power series. As a result, the Weierstrass preparation theorem shows that the fold point in the (κ,ω) plane occurring in the spectral-gap region as discussed by *Yakovlev and Hanson* [1997] is a sufficient condition for the determination of a branch point in the ω plane defined by equations (5) and (6). Note that the condition $H''_{\kappa\kappa} \neq 0$ is not implied by the Weierstrass theorem but comes from the definition of the fold point. Note also that the condition $H'_\omega \neq 0$ is a sufficient but not necessary condition.

For completeness, considering the Morse critical point (MCP) (κ_m,ω_m), discussed by*Yakovlev and Hanson* [1997, and references therein], and *Shestopalov and Shestopalov* [1996], which occurs in the mode coupling region, the following conclusions can be made. It has been shown that the MCP is defined by the following set of equations:

$$H'_\kappa(\kappa,\omega)|_{(\kappa_m,\omega_m)} = H'_\omega(\kappa,\omega)|_{(\kappa_m,\omega_m)} = 0 ,$$
$$\xi = [H''_{\kappa\kappa}H''_{\omega\omega} - H''_{\kappa\omega}H''_{\omega\kappa}]|_{(\kappa_m,\omega_m)} \neq 0 . \quad (15)$$

It can be seen that the condition $H'_\omega(\kappa_m,\omega_m) \neq 0$ is not satisfied, which represents an important condition in the definition of a branch point.

Also, it can be observed that the local structure $\kappa = \kappa(\omega)$ obtained in the vicinity of the MCP (κ_m,ω_m) [*Yakovlev and Hanson*, 1998]

$$\kappa_{1,2} = \kappa_m - \frac{H''_{\kappa\omega}}{H''_{\kappa\kappa}}(\omega - \omega_m) \pm \frac{\sqrt{((H''_{\kappa\omega})^2 - H''_{\kappa\kappa}H''_{\omega\omega})(\omega - \omega_m)^2 - 2H''_{\kappa\kappa}H}}{H''_{\kappa\kappa}} \quad (16)$$

does not indicate that $\omega = \omega_m$ is a branch point in the ω plane due to presence of the term $(\omega - \omega_m)^2$ if $H = 0$ as in a degenerate MCP, and a nondegenerate MCP does not lie on the dispersion curve and so it cannot represent a branch point.

The determination of ω-plane branch points of the dispersion function $\kappa(\omega)$ will be shown for the examples of a parallel-plate waveguide, a grounded dielectric slab waveguide, and aprinted transmission line. The parallel-plate waveguide is included here since it admits an entirely analytical investigation. The grounded slab and printed transmission line geometries represent structures with increasingly complicated characteristic determinants $H(\kappa,\omega)$. In all examples, an $e^{j(\omega t - \kappa z)}$ dependence will be assumed and suppressed.

2.1. Parallel-Plate Waveguide

Consider a parallel-plate waveguide geometry shown in the inset of the top panel of Figure 1. The structure is uniform in the xz plane and filled by a medium with real material parameters (although this is not a necessary restriction). Assuming the propagation of transverse electric (TE) and transverse magnetic (TM) modes in the axial z direction, the following characteristic eigenvalue equation can be obtained:

$$H(\kappa,\omega) = \sinh\left(\sqrt{\kappa^2 - k^2}2h\right) = 0 \quad (17)$$

which immediately results in the representation for the propagation constant $\kappa(\omega)$

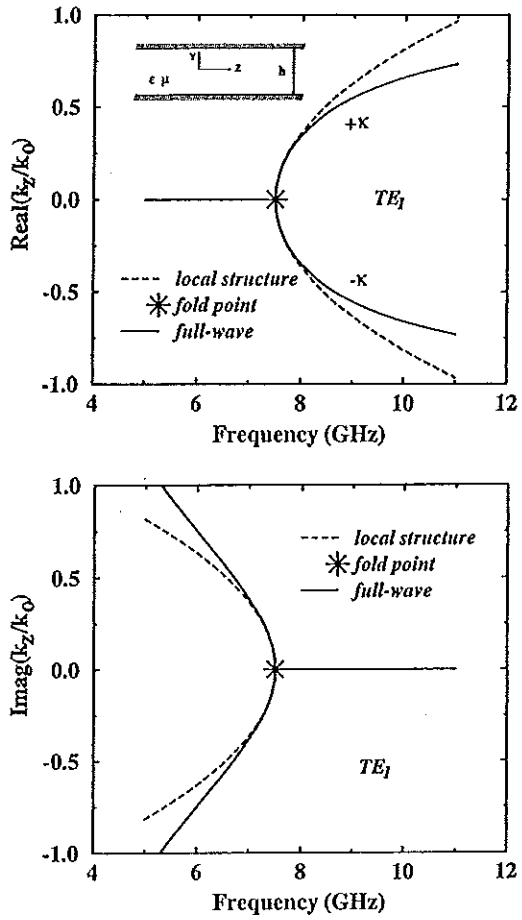

Figure 1. Dispersion behavior for the TE_1 (transverse electric) mode of a parallel-plate waveguide, $\epsilon = \epsilon_0$, $\mu = \mu_0$, and $h = 1$ cm. Local structure is generated in the vicinity of the fold point.

$$\kappa(\omega) = \pm\sqrt{k^2 - \left(\frac{n\pi}{2h}\right)^2}, \quad n = 0, \pm1, \pm2, \pm3, \ldots \tag{18}$$

where $k = \omega\sqrt{\epsilon\mu}$.

The propagation constant expression (equation (18)) leads to the following result for propagating and evanescent modes:

$$\kappa_{\text{real}}(\omega) = \pm\sqrt{k^2 - \left(\frac{n\pi}{2h}\right)^2} \quad \omega > \left(\frac{n\pi}{2h}\right)\frac{1}{\sqrt{\epsilon\mu}}$$

$$\kappa_{\text{imag}}(\omega) = \mp j\sqrt{\left(\frac{n\pi}{2h}\right)^2 - k^2} \quad \omega < \left(\frac{n\pi}{2h}\right)\frac{1}{\sqrt{\epsilon\mu}} \tag{19}$$

respectively. Clearly, the cutoff frequencies ω_c are determined for $\kappa(\omega) = 0$, leading to the formula

$$\omega_c = \left(\frac{n\pi}{2h}\right)\frac{1}{\sqrt{\epsilon\mu}}. \tag{20}$$

It is easily seen that the cutoff frequencies ω_c simultaneously represent branch point types ω_0 and ω_1 in the ω plane. Observe from (4)

$$H(0, \omega_0) = \sin(2kh) = 0$$

resulting in the formula for the point ω_0

$$\omega_0 = \left(\frac{n\pi}{2h}\right)\frac{1}{\sqrt{\epsilon\mu}}. \tag{21}$$

As a check on the other conditions (5),

$$H(\kappa_1, \omega_1) = \sinh\left(\sqrt{\kappa_1^2 - k_1^2}2h\right) = 0$$

$$\Longrightarrow \quad \kappa_1(\omega_1) = \pm\sqrt{k_1^2 - \left(\frac{n\pi}{2h}\right)^2} \tag{22}$$

$$H'_\kappa(\kappa_1, \omega_1) = \frac{(2\kappa_1 h)\cosh\left(\sqrt{\kappa_1^2 - k_1^2}2h\right)}{\sqrt{\kappa_1^2 - k_1{}^2}} = 0$$

$$\Longrightarrow \quad \kappa_1 = 0. \tag{23}$$

Also, it can be proved that $H'_\omega H''_{\kappa\kappa} \neq 0$ at $\omega = \omega_f$ and $\kappa_f = 0$

$$H'_\omega(\kappa_f, \omega_f)|_{\kappa_f=0} =$$

$$= \frac{(-2k_f h)\cosh\left(\sqrt{\kappa_f^2 - k_f^2}2h\right)}{\sqrt{\kappa_f^2 - k_f^2}}|_{\kappa_f=0} \neq 0 \tag{24}$$

$$H''_{\kappa\kappa}(\kappa_f, \omega_f)|_{\kappa_f=0} =$$

$$= \frac{(-2k_f^2 h)\cosh\left(\sqrt{\kappa_f^2 - k_f^2}2h\right)}{(\kappa_f^2 - k_f^2)^{3/2}}|_{\kappa_f=0}$$

$$+\frac{(2\kappa_f h)^2\sinh\left(\sqrt{\kappa_f^2 - k_f^2}2h\right)}{(\kappa_f^2 - k_f^2)}|_{\kappa_f=0} \neq 0, \tag{25}$$

where $k_1 = k(\omega_1)$, $k_f = k(\omega_f)$.

Comparison of equations (20) and (21) with (22)-(25) shows that $\omega_c = \omega_0 = \omega_1$. Regarding the zero cutoff frequency for the dominant TM_0

mode, it is clear from (18) that for $n = 0$ a branch point does not occur in the ω plane due to the presence of the ω^2 term. The dispersion function $\kappa(\omega)$ for this dominant mode, which is actually a TEM mode, is an entire function of frequency. Every other mode has branch points at $\omega = \omega_0 = \omega_c$. In the event of material loss, all modes, including the dominant mode, have branch points associated with the conductivity of the medium.

For the specific example of a parallel-plate waveguide it is determined that the cutoff frequencies ω_c for all but the dominant mode represent branch points of the dispersion function in the ω plane, and $\omega_0 = \omega_1 = \omega_c$. This indicates that at ω_c the curves $\kappa, -\kappa$ (κ, κ^* trivially) come together.

Numerical study of the branch point $f_0 = f_1 = f_c$ ($f = \omega/2\pi$) associated with the fold point is provided in Figure 1. In this figure and in all subsequent figures, the longitudinal wavenumber κ is replaced by k_z. The fold point in the (κ, f) plane with coordinates $(0, 7.5)$ has been obtained from the numerical solution of equations (5) and (6), where κ and f are in units of centimeters and gigahertz, respectively. The local structure shown in Figure 1 has been generated using a Taylor series expansion in the vicinity of the fold point [see *Yakovlev and Hanson*, 1997, equation (5)], and the full-wave results come from (19). Very good agreement with full-wave dispersion behavior is observed in a local region. This behavior is also represented by normal forms (equation (7)), which provide a qualitative description of dispersion characteristics.

2.2. Grounded Dielectric Slab Waveguide

As a second example, consider a grounded dielectric slab waveguide configuration demonstrated in the inset in Figure 2. The structure is uniform in the xz plane and characterized by material parameters ϵ_1 and ϵ_2 representing permittivities of the cover and slab, respectively. The solution of the Helmholtz equation

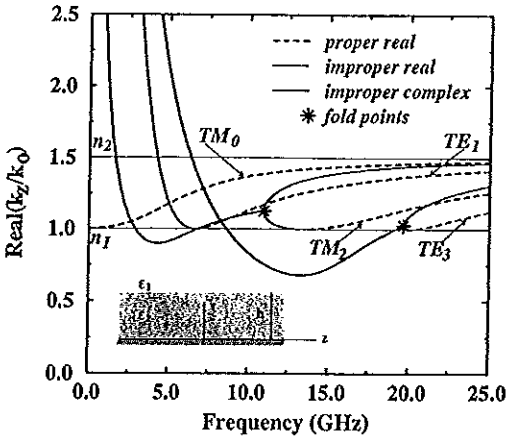

Figure 2. Dispersion behavior of dominant and higher order TE-odd and TM-even modes in a grounded dielectric slab waveguide, $h = 1$ cm, $\epsilon_1 = \epsilon_0$, and $\epsilon_2 = 2.25\epsilon_0$.

with boundary conditions on the ground surface and continuity conditions for tangential components of the electric field on the surface of the interface can be obtained for TE^z-odd and TM^z-even modes, leading to the eigenvalue equations [*Collin*, 1991] with the characteristic functions

$$H^{\mathrm{TE}}(\kappa, \omega) = \gamma_1 + \gamma_2 \coth(\gamma_2 h)\,,$$
$$H^{\mathrm{TM}}(\kappa, \omega) = \gamma_1 + \frac{n_1^2}{n_2^2}\gamma_2 \tanh(\gamma_2 h) \qquad (26)$$

where $n_1 = \sqrt{\epsilon_1/\epsilon_0}$, $n_2 = \sqrt{\epsilon_2/\epsilon_0}$, and

$$\gamma_{1,2} = \pm\sqrt{\kappa^2 - n_{1,2}^2 k_0^2}\,, \quad k_0 = \frac{\omega}{c}\,, \quad c = \frac{1}{\sqrt{\epsilon_0\mu_0}}\,.$$

The square root associated with γ_1 necessitates the definition of branch cuts in the κ plane, while no such cuts are necessary for γ_2, since both terms in (26) are even in γ_2. The standard hyperbolic cuts defined by $\mathrm{Re}\{\gamma_1\} = 0$ are used here, separating modes that decrease (proper) and increase (improper) away from the slab.

It has been shown that the branch point ω_0 occurs in the ω plane to separate $(\kappa, -\kappa)$ solutions and satisfies (4) and (6). Considering the above characteristic function for TE-odd and TM-even modes, the coordinates of ω_0 branch points can be easily determined analytically. Equation (4)

applied to either term in (26) leads to

$$\tan(n_2 k_0 h) = \pm j \frac{n_2}{n_1}, \qquad (27)$$

which can be inverted to yield

$$\omega_0 = \pm\left(\frac{n\pi}{2}\right)\frac{c}{n_2 h} \pm j\frac{c}{2n_2 h}\ln\left[\frac{\frac{n_2}{n_1}+1}{\frac{n_2}{n_1}-1}\right], \quad n = 1,3,5,\ldots \qquad (28)$$

where all four sign combinations are necessary. It can be shown that the values of the index n are associated with modes as (TM_{n+1},TE_n). Here we index the modes according to the order of cutoff frequency in a symmetric slab waveguide. Only the even TM modes of the symmetric-slab waveguide of thickness $2h$ may propagate on the grounded slab waveguide of thickness h considered here, denoted with an even subscript, while only the odd TE modes may propagate on the grounded slab waveguide, denoted with an odd subscript. Note that the ω_0 branch points are symmetrically located in the four quadrants of the ω plane and that they lead to κ values on the improper Riemann sheet of the κ plane.

For the grounded slab, ω_1 branch points defined by (5) and (6) separating (κ, κ^*) cannot be evaluated analytically. Although (5) and (6) represent two simultaneous nonlinear equations in two unknowns, it can be shown that at ω_1, $\gamma_1 h = -1$ for the TE modes [*Yamaguchi et al.*, 1990]. This reduces the numerical work to solving

$$H^{TE}(\kappa, \omega_1)\big|_{\kappa=\sqrt{1/h^2+(n_1\omega_1/c)^2}} = 0 .$$

No such simplification is available for the TM modes.

Dispersion characteristics of TE-odd and TM-even modes are shown in Figure 2 for the real part of the normalized propagation constant k_z/k_0. It is widely known in the literature, for example, *Collin* [1991], that leakage of higher-order modes occurs in slab waveguides. Theoretical and numerical investigation of the dominant TM_0 mode shows that this mode never leaks energy into the cover region. It can be observed that the first odd-mode TE_1 does not leak either, but an improper real solution occurs below the cutoff frequency for this mode. (The cutoff frequency of a proper mode in an open waveguide is defined as the frequency for which the mode changes from the proper Riemann sheet of the κ plane to the improper sheet. This occurs at the spatial transform branch point $\kappa = n_1 k_0$ or on its associated cut.) It can be seen that starting with the second higher mode, TM_2, leakage (radiation) exists in dielectric slab waveguide. The spectral-gap region is formed by a pair of improper real solutions and a conjugate pair of complex (leaky mode) solutions. Qualitative behavior of dispersion curves in the spectral-

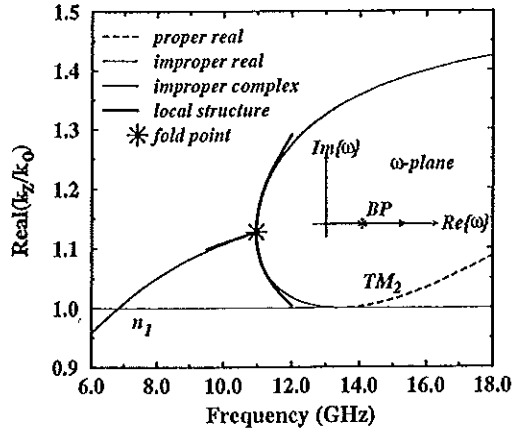

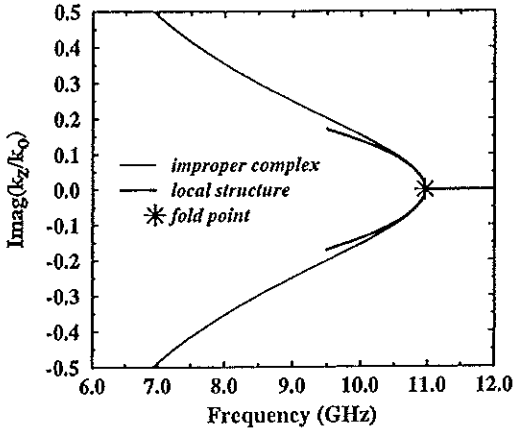

Figure 3. Dispersion propagation constant characteristics for the TM_2 mode and the local structure generated in the vicinity of the fold point. Inset shows the path of frequency variation.

gap region is similar to that observed for various printed transmission line circuits [*Yakovlev and Hanson*, 1997; *Shigesawa et al.*, 1995]. Fold points have been found in the $\kappa - f$ plane at the intersection of improper real and complex solutions for the higher-order modes starting at TM_2, as demonstrated in Figure 2. Figure 3 demonstrates dispersion propagation constant characteristics for the TM_2 mode in the region of interest and the local structure generated in the vicinity of the fold point using a Taylor series expansion. The inset in Figure 3 shows the path in the frequency plane over which frequency is varied. It can be observed that qualitative and quantitative dispersion behavior in the localized spectral-gap region is completely determined by characteristics of the fold point.

Figure 4 and Figure 5 demonstrate the location of ω_0- and ω_1-type frequency plane branch points for corresponding TM-even and TE-odd modes of the grounded dielectric slab waveguide. The coordinates of f_0 points for (TM_{n+1},TE_n) modes are $(\pm n5, \pm 2.5615)$ GHz, $n = 1, 3, 5, \ldots$ from (29) such that these branch points occur in conjugate pairs. The solid curve $\mathrm{Re}\{\kappa\} = 0$ separates (Re{κ}, -Re{κ}) solutions and can be chosen as a physically meaningful branch cut (separating the forward from the backward propagating modes). It can be confirmed that equations (5) and (6) are satisfied at these points. Note that the singularities in the upper half (lower half) frequency plane correspond to complex modes that decrease (increase) along the waveguiding axis.

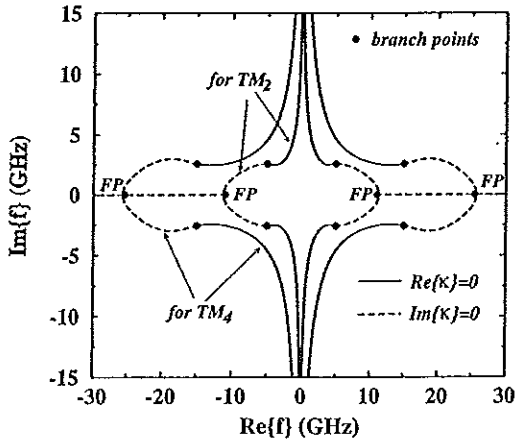

Figure 4. Frequency-plane branch points for TM_2 and TM_4 even modes. The curves $\mathrm{Re}\{\kappa\} = 0$ can be chosen as appropriate branch cuts. Points on the real axis are of ω_1-type, while those off of the real axis are of ω_0-type.

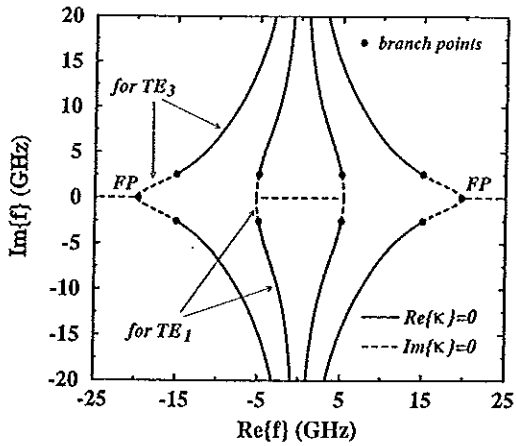

Figure 5. Frequency-plane branch points for TE_1 and TE_3 odd modes. The branch point f_1 does not occur for the TE_1 mode.

The coordinates of the f_1-type branch points (on the real-frequency axis) must be determined numerically. For the TM_2, TE_3, and TM_4 modes, the fold point coordinates (κ, f) are $(1.1275, 10.9648)$, $(1.0291, 19.6589)$, and $(1.0495, 25.3669)$, respectively.

The curve $\mathrm{Im}\{\kappa\} = 0$ separates (Im{κ}, -Im{κ}) solutions and is shown for convenience, but it does not indicate an appropriate branch cut separating modes in the (κ, f) plane. The horizontal dashed-line segments emanating from the ω_1 branch points and directed outward could be considered as a meaningful branch cut, a section of which separates modes from their conjugates. Note that the TM_0 mode does not possess ω_0 or ω_1-type branch points and the TE_1 mode does not possess ω_1-type branch points. All higher-order modes beyond TE_1 possess both types of branch points and behave in a qualitatively similar manner. For these higher-order modes, the two improper real solutions exist on different frequency plane Riemann sheets, in that a complete revolution in the complex

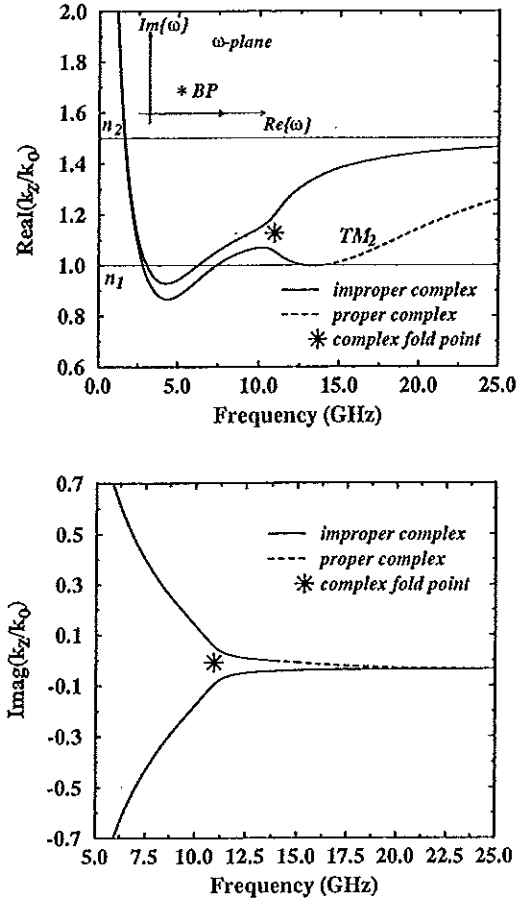

Figure 6. Dispersion behavior for TM_2 mode of a lossy grounded dielectric slab waveguide, $h = 1$ cm, $\epsilon_1 = \epsilon_0$, and $\epsilon_2 = (2.25 - \jmath 0.1)\epsilon_0$. Inset shows the path of frequency variation.

frequency plane around a ω_1-type branch point shows an analytically continuous transition from one improper real solution to the other. Similar comments apply to the complex conjugate solutions. The $\mathrm{Re}(\kappa) = 0$ ($\mathrm{Im}(\kappa) = 0$) curves in Figures 4 and 5 were obtained numerically by starting at the appropriate branch point, increasing κ as $(0, \kappa_i)$ $((\kappa_r, 0))$, and performing a root search for the complex frequency which provides those values.

The concept of the ω_1-type branch point is especially useful for interpreting the spectral-gap behavior in the presense of loss. Consider a lossy grounded slab waveguide with the complex permittivity $\epsilon_2 = (2.25, -\jmath 0.1)\epsilon_0$ and the same geometrical parameters as in the previous example. Dispersion characteristics for the TM_2 even mode are demonstrated in Figure 6. In comparison with the lossless case it can be seen that the conjugate complex (leaky mode) solutions split into two complex modes, and the classical dispersion behavior in the spectral-gap region no longer exists. The complex fold point with coordinates $(\kappa, f) = (1.1276 - \jmath 0.00989, 10.9317 + \jmath 0.5422)$ has been found, which determines a complex ω_1-type branch point in the frequency plane, as the real fold point indicated for lossless media. To obtain a bifurcation of solutions at the fold point (branch point in the frequency plane), consider a complex variable frequency with the same imaginary part as in the fold point frequency: $\mathrm{Im}\{f\} = 0.5422$ GHz. Propagation

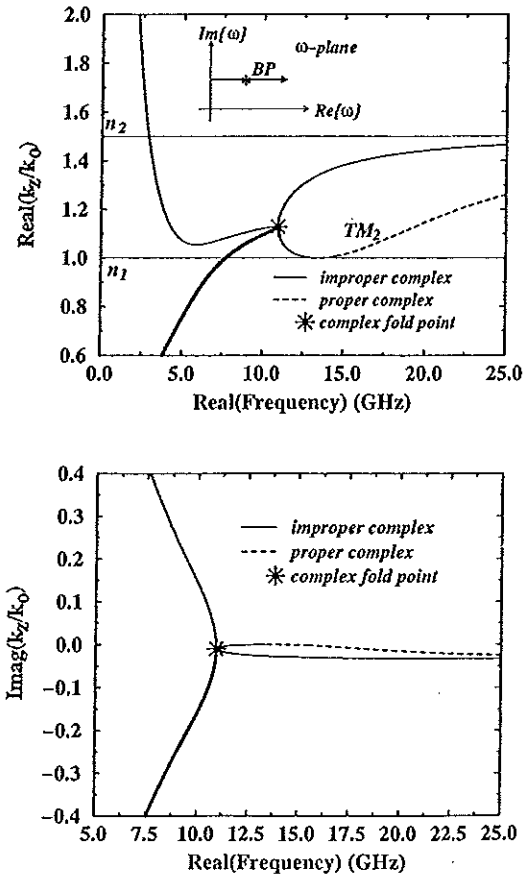

Figure 7. Propagation constant characteristics for the TM_2 mode versus complex frequency with $\mathrm{Im}\{f\} = 0.5422$ GHz. Bifurcation of solutions occurs at the complex fold point. Inset shows the path of frequency variation.

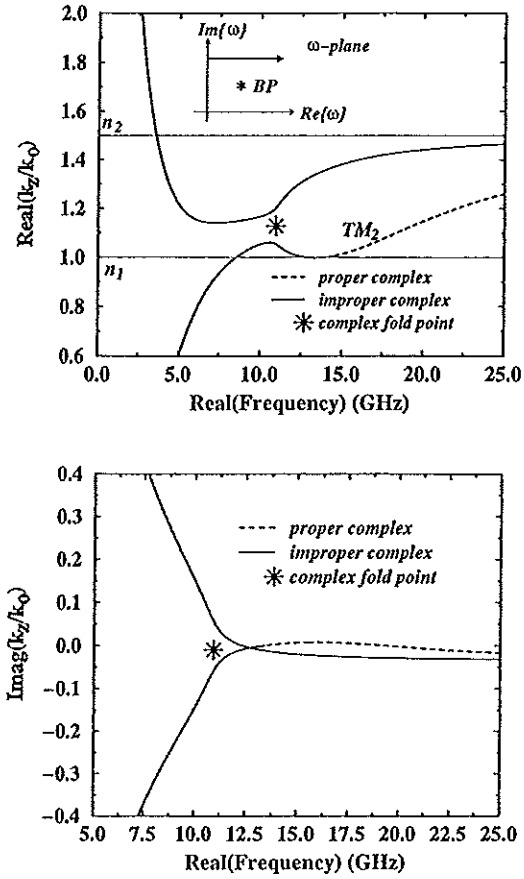

Figure 8. Propagation constant characteristics for the TM_2 mode versus complex frequency with $\mathrm{Im}\{f\} = 1$ GHz. Bifurcation of solutions does not occur at the complex fold point. Inset shows the path of frequency variation.

constant characteristics for the TM_2 even mode versus the real part of the complex frequency, with constant imaginary part, are shown in Figure 7. It can be observed that the bifurcation of solutions occurs at the complex fold point determined above, demonstrating that the complex fold point obtained in a lossy case represents the complex branch point ω_1 defined by equations (5) and (6). Note that conjugate modes no longer exist, due to the complex frequency used. Figure 8 shows propagation constant characteristics for a lossy slab waveguide versus complex frequency with $\mathrm{Im}\{f\} = 1$ GHz, i.e., along a complex frequency contour above the branch point. It should be noted that the bifurcation of solutions in the (κ, f) plane occurs only in the case when the frequency path crosses the f-plane branch point along any such frequency plane contour.

Examination of Figure 6 shows that when frequency is varied along a path below the ω_1-type branch point, the proper bound mode (complex due to $\mathrm{Im}(\omega) \neq 0$ or $\mathrm{Im}(\epsilon) \neq 0$ or both) is analytically continuous with the improper nonphysical below-cutoff complex mode, and the improper mode (which is the improper real mode for $\mathrm{Im}(\omega)$=$\mathrm{Im}(\epsilon) = 0$) is analytically continuous with the improper physical below-cutoff complex mode. Figure 8 shows that when frequency is varied along a path above the ω_1-type branch point, the reverse situation occurs. This was first observed by *Haddon* [1986] and has impor-

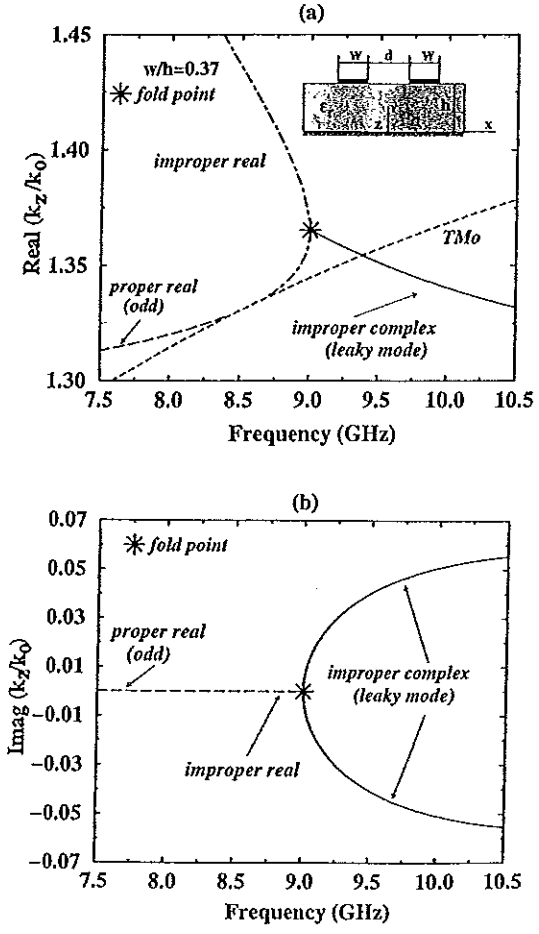

Figure 9. Dispersion behavior of improper real and complex modes in the spectral gap region of a conductor-backed coplanar strip line, $h = 1$ cm, $\epsilon_r = 2.25$, and $d/h = 0.25$.

tant implications for computing the response of a slab waveguide using leaky modes.

2.3. Conductor-Backed Coplanar Strip Line

In the third example, a full-wave analysis of a conductor-backed coplanar strip line geometry shown in the inset of Figure 9 has been performed using an electric-field integral equation technique, as was used by *Yakovlev and Hanson* [1997]. A coupled set of homogeneous integral equations has been obtained, enforcing the boundary condition for the tangential component of the electric field on the surface of the conducting strips. Dispersion propagation constant characteristics have been determined from the numerical solution of a coupled integral equation system with unknown current density expanded as a series of Chebyshev polynomials. Full-wave results for proper and improper modes in a conductor-backed coplanar strip line have been demonstrated and discussed by *Yakovlev and Hanson* [1997], using the concept of critical fold and Morse points. In this section, dispersion behavior of all possible solutions will be shown in some local regions (spectral-gap) wherein the branching of solutions occurs.

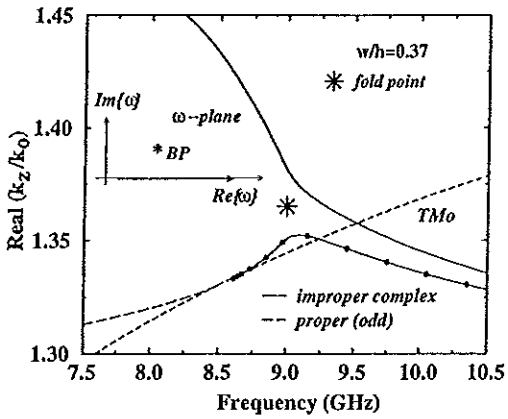

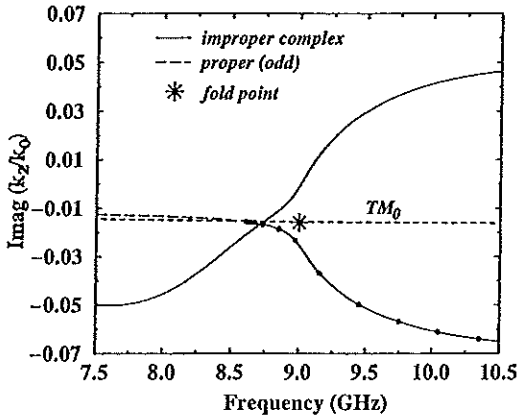

Figure 10. Dispersion behavior for improper complex modes of a lossy conductor-backed coplanar strip line, $h = 1$ cm, $d/h = 0.25$, and $\epsilon_r = 2.25 - j0.05$. Inset shows the path of frequency variation.

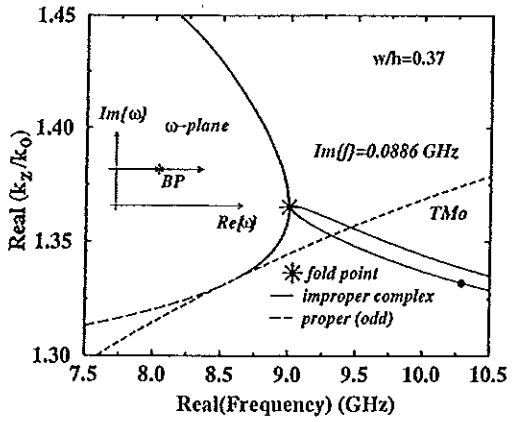

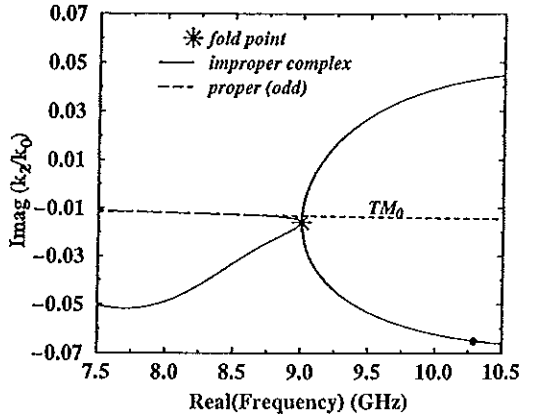

Figure 11. Propagation constant characteristics for improper complex modes versus frequency with $\mathrm{Im}\{f\} = 0.0886$ GHz. Branching of solutions occurs at the complex fold point. Inset shows the path of frequency variation.

Dispersion characteristics for improper real and improper complex (leaky mode) solutions for the dominant odd mode in the spectral-gap region are demonstrated in Figure 9. Dispersion characteristic behavior in the vicinity of

the intersection point is formed by two real solutions which resemble branches of a parabola and a complex solution which resembles a straight line in a similar manner to the grounded slab modes just below cutoff. It has been discussed previously that the intersection point within the spectral-gap region is a fold point. For the specific example, the fold point with coordinates $(\kappa, f) = (1.3654, 9.0028)$ has been determined, as shown in Figure 9. The fold point in the (κ, f) plane represents the frequency-plane branch point ω_1 separating (κ, κ^*) solutions. Note that the lower improper real mode in Figure 9a, which becomes tangent to the TM_0 background mode, eventually becomes a proper real (odd) mode upon further decreasing of frequency [see also *Shigesawa et al.*, 1995].

Consider a lossy conductor-backed coplanar strip line configuration with the complex permittivity of the substrate $\epsilon_r = (2.25, -j0.05)$ and the same geometrical parameters as in the lossless example. Dispersion behavior of improper complex solutions is demonstrated in Figure 10. It can be seen that the propagation constant characteristics are significantly changed and the classical dispersion behavior in the spectral-gap region no longer exists [*Shigesawa et al.*, 1993], similar to the example of a lossy grounded dielectric slab waveguide. The complex fold point has been found with coordinates $(\kappa, f) = (1.3652 - j0.0159, 8.9999 + j0.0886)$, the frequency of which is associated with the complex ω_1 branch point in the frequency plane. As in the example for a lossy slab waveguide, consider a complex variable frequency having constant imaginary part $\mathrm{Im}\{f\} = 0.0886$ GHz. Propagation constant characteristics of improper complex modes versus complex frequency with the same imaginary part as in the fold point frequency are shown in Figure 11. It can be seen that branching of solutions occurs at the complex fold point, indicating that the complex fold point frequency determines in a lossy structure the complex branch point f_1 in the frequency plane separating two complex modes $(\kappa, \tilde{\kappa}^*)$ that would be a conjugate pair in the lossless case. Figure 12 shows

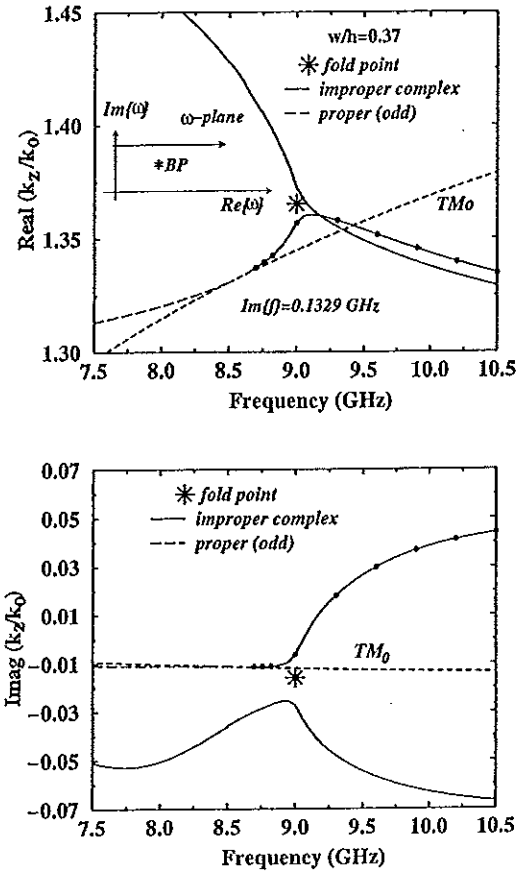

Figure 12. Propagation constant characteristics for improper complex modes versus frequency with $\mathrm{Im}\{f\} = 0.1329$ GHz. Inset shows the path of frequency variation.

the corresponding case for a frequency path above the fold point. Comparing Figures 10 and 12, when the frequency path passes below the fold point (Figure 10), the physically meaningful leaky mode is continuous with the mode which becomes proper as frequency is lowered, whereas if the frequency path passes above the fold point (Figure 12) it is the nonphysical leaky-mode which becomes the proper mode as frequency is lowered. Note that for the dielectric slab, the opposite behavior occurs, although in this case the modes become proper as frequency is increased rather than decreased.

It has been discussed by *Yakovlev and Hanson* [1997] that parameterization of the propagation constant characteristics by strip width parameter w/h leads to migration and trans-

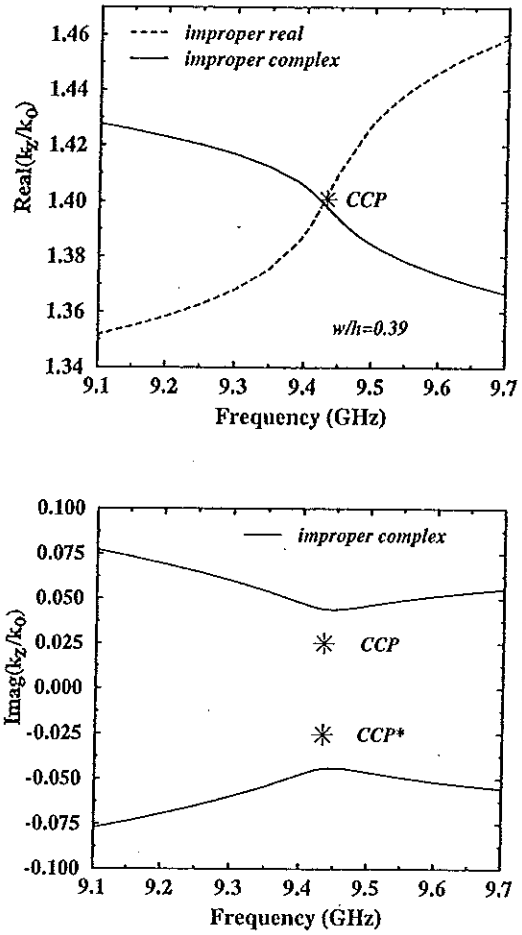

Figure 13. Dispersion behavior for improper real and complex modes of a conductor-backed coplanar strip line, $h = 1$ cm, $d/h = 0.25$, and $\epsilon_r = 2.25$.

formation of critical points. For example, the transformation of real-valued fold points (FPs) 1 and 2 into complex conjugate points (CCPs) appears at a singular point B, which is found within the range 0.3855 and 0.3856 of w/h values (see Figures 6 and 7 of *Yakovlev and Hanson* [1997] and associated discussion). Dispersion behavior of improper real and improper complex modes for $w/h = 0.39$ (just after singular point B) is demonstrated in Figure 13 for a lossless conductor-backed coplanar strip line configuration. It can be seen that the conjugate pair of complex critical points (CCPs) has been found with coordinates $(1.4008 \pm j0.0253, 9.4328 \pm j0.0348)$. It can be shown that the complex conjugate critical points represent the complex conjugate frequency plane branch points ω_1 defined by equations (5) and (6).

As in the previous examples, which consider complex fold points, we will transform the frequency plane coordinate system. The full-wave results have been generated for the same material and geometrical parameters of the structure versus complex frequency with a conjugate pair of imaginary parts. To show the branching of solutions, consider the constant imaginary parts equal to those in the complex fold point frequencies: $\mathrm{Im}\{f\} = \pm 0.0348$ GHz. Dispersion behavior of improper complex solutions with a complex frequency considered is shown in Figure 14. Bifurcation of solutions occurs at complex conjugate points (complex fold points) determined previously. The results shown in Figure 14 explicitly demonstrate that a conju-

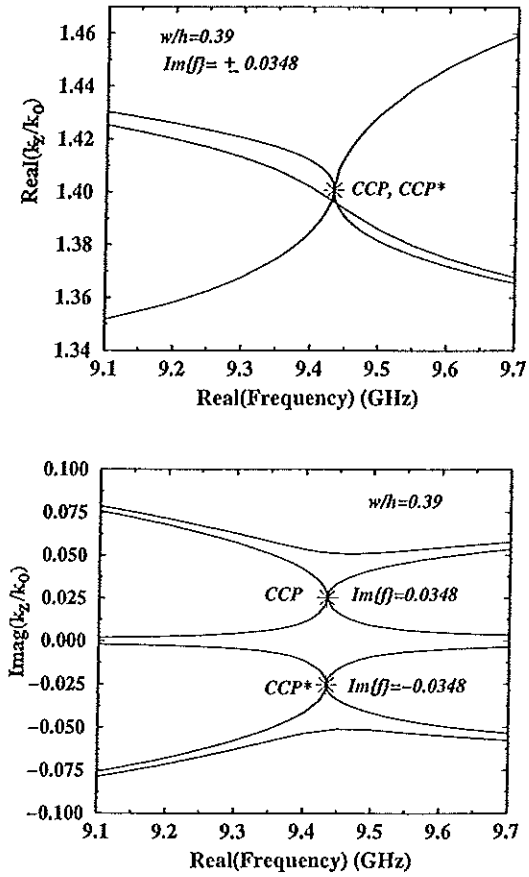

Figure 14. Propagation constant characteristics for improper complex modes versus frequency with $\mathrm{Im}\{f\} = \pm 0.0348$ GHz.

gate pair of complex fold points obtained in a lossless structure is associated with a conjugate pair of frequency-plane complex branch points ω_1 defined by equations (5) and (6). Thus it is concluded that all of the various real and complex fold points described by *Yakovlev and Hanson* [1997] indicate frequency-plane branch points of the ω_1 type.

The qualitative and quantitative dynamic behavior of a conductor-backed coplanar strip line has been investigated by examining the evolution of different critical points (fold and Morse points) versus strip width parameter w/h, and presented [see *Yakovlev and Hanson*, 1997, Figures 6 and 7]. It has been shown that changes in the types of critical points are related to qualitative changes of structural characteristics of a system. The analysis presented here shows that different types of critical points, including real, complex, and complex conjugate fold points, are associated with corresponding frequency plane real and complex branch points separating complex solutions. The evolution of real and complex ω_1 branch points versus strip width has been generated showing possible transformations of those points related to appearance and disappearance of leakage regimes. Figure 15 demonstrates the evolution of branch points (BPs) related to the evolution of critical points shown in Figures 6 and 7 of *Yakovlev and Hanson* [1997] for a coplanar strip line. It should be noted that complex conjugate points BP1 and BP3, associated with complex conjugate points CCP1 and CCP3, transform into real branch points BP1 and BP3 at singular point A, which occurs between $w/h = 0.37040$ and $w/h = 0.37045$.

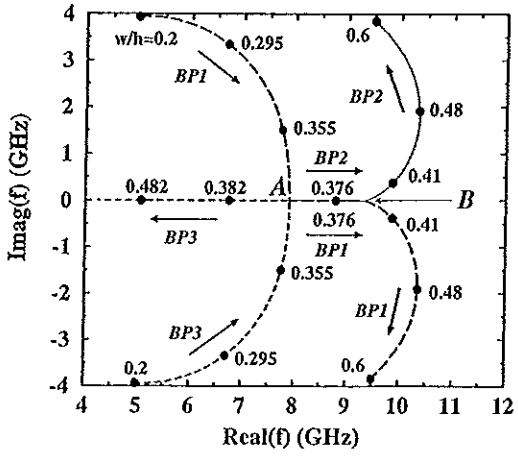

Figure 15. The evolution of real and complex frequency plane branch points versus strip width parameter w/h.

The transformation of real branch points BP1 and BP2, associated with real fold points FP1 and FP2, into complex conjugate points BP1 and BP2 occurs at singular point B, which is found within the range of 0.3855 and 0.3856 of w/h values. Taken together, Figures 6 and 7 of *Yakovlev and Hanson* [1997] and Figure 15 here show the complete dynamical evolution of relevant critical points parameterized by strip width in the temporal and spatial transform planes.

3. Conclusion

The investigation of frequency-plane branch points found in various guided-wave structures, including a parallel-plate waveguide, a grounded dielectric slab waveguide, and a conductor-backed coplanar strip line, is presented. On the basis of the normal form of a fold point and the Weierstrass preparation theorem, it is analytically shown that frequency-plane branch points separating conjugate dispersion solutions satisfy the general formulation given previously for fold points in the spectral-gap region. Additional branch points separating positive and negative dispersion solutions are obtained for the examples of a parallel-plate waveguide and a grounded dielectric-slab waveguide. It is shown that real, complex, and complex conjugate fold points are associated with frequency-plane real, complex, and complex conjugate branch points, respectively. The evolution of real and complex branch points versus strip width for conductor-backed coplanar strips has been generated, showing transformations of those points related to existence, appearance, and disappearance of leakage.

Acknowledgments. The authors acknowledge helpful discussions with Hans Volkmer from the Department of Mathematical Sciences, University of Wisconsin-Milwaukee.

References

Bagby, J.S., C.H. Lee, D.P. Nyquist, and Y. Yuan, Identification of propagation regimes on integrated microstrip transmission lines, *IEEE Trans. Microwave Theory Tech.*, *41*, 1887-1893, 1993.

Barkeshli, S., P.H. Pathak, and M. Marin, An asymptotic closed form microstrip surface Green's function for the efficient moment method analysis of mutual coupling in microstrip antennas, *IEEE Trans. Antennas Propag.*, *38*, 1374-1383, 1990.

Blok, H., J.M. Van Splunter, and H.G. Janssen, Leaky-wave modes and their role in the numerical evaluation of the field excited by a line source in a non-symmetric, inhomogeneously layered, slab waveguide, *Appl. Sci. Res.*, *41*, 223-236, 1984.

Bochner, S., and W.T. Martin, *Several Complex Variables*, Princeton Univ. Press, Princeton, N.J., 1948.

Carpentier, M.P., and A.F. dos Santos, Nonspectral representation of the field of a horizontal wire above ground, *Radio Sci.*, *19*(3), 812-828, 1984.

Carpentier, M.P., and A.F. dos Santos, Non-spectral complete field expansion in two-dimensional structures, *IMA J. Appl. Math.*, *35*, 1-12, 1985.

Collin, R.E., *Field Theory of Guided Waves*, 2nd. ed., IEEE Press, Piscataway, N.J., 1991.

Duffy, D.G., Response of a grounded dielectric slab to an impulse line source using leaky modes, *IEEE Trans. Antennas Propag.*, *42*, 340-346, 1994.

Golubitsky, M., and D.G. Schaeffer, *Singularities and Groups in Bifurcation Theory*, vol. 1, Springer-Verlag, New York, 1985.

Haddon, R.A.W., Exact evaluation of the response of a layered elastic medium to an explosive point source using leaking modes, *Bull. Seismol. Soc. Am.*, *76*(6), 1755-1775, 1986.

Haddon, R.A.W., Response of an oceanic wave guide to an explosive point source using leaking modes, *Bull. Seismol. Soc. Am.*, *77*(5), 1804-1822, 1987a.

Haddon, R.A.W., Numerical evaluation of Green's functions for axisymmetric boreholes using leaking modes, *Geophysics*, *52*(8), 1099-1105, 1987b.

Haddon, R.A.W., Exact Green's functions using leaking modes for axisymmetric boreholes in solid elastic media, *Geophysics*, *54*(5), 609-620, 1989.

Jackson, D.R., and A.A. Oliner, A leaky-wave analysis of the high-gain printed antenna configuration, *IEEE Trans. Antennas Propag.*, *36*, 905-910, 1988.

Marcuvitz, N., On field representation in terms of leaky modes or eigenmodes, *IRE Trans.*, *AP-4*, 192-194, 1956.

Nghiem, D., J.T. Williams, D.R. Jackson, and A.A. Oliner, Existence of a leaky dominant mode on microstrip line with an isotropic substrate: Theory and measurements, *IEEE Trans. Microwave Theory Tech.*, *44*, 1710-1715, 1996.

Oliner, A.A., Leakage from various waveguides in millimeter wave circuits, *Radio Sci.*, *22*(6), 866-872, 1987a.

Oliner, A.A., Leakage from higher modes on microstrip line with application to antennas, *Radio Sci.*, *22*(6), 907-912, 1987b.

Seydel, R., *Practical Bifurcation and Stability Analysis*, 2nd ed., Springer-Verlag, New York, 1994.

Shestopalov, V.P., and Y.V. Shestopalov, *Spectral Theory and Excitation of Open Structures*, Inst. of Electr. Eng., London, 1996.

Shigesawa, H., M. Tsuji, and A.A. Oliner, Conductor-backed slot line and coplanar waveguide: Dangers and full-wave analyses, in *1988 IEEE/MTT-S International Microwave Symposium Digest, G-2*, pp. 199-202, Ins. of Electr. and Electron. Eng., New York, 1988.

Shigesawa, H., M. Tsuji, and A.A. Oliner, Dominant mode power leakage from printed-circuit waveguides, *Radio Sci.*, *26*(2), 559-564, 1991.

Shigesawa, H., M. Tsuji, and A.A. Oliner, The nature of the spectral-gap between bound and leaky solutions when dielectric loss is present in printed-circuit lines, *Radio Sci.*, *28*(6), 1235-1243, 1993.

Shigesawa, H., M. Tsuji, and A.A. Oliner, Simultaneous propagation of bound and leaky dominant modes on printed-circuit lines: A new general effect, *IEEE Trans. Microwave Theory Tech.*, *43*, 3007-3019, 1995.

Tamir, T., Wave-number symmetries for guided complex waves, *Electron. Lett.*, *3*(5), 180-182, 1967.

Tamir, T., and A.A. Oliner, Guided complex waves, *Proc. Inst. Electr. Eng.*, *110*(2), 310-334, 1963.

Tesler, M.H., and G. Eichmann, Non-spectral field representations in dielectric fiber guides, *J. Inst. Math. Its Appl.*, *21*, 315-330, 1978.

Yakovlev, A.B., and G.W. Hanson, On the nature of critical points in leakage regimes of a conductor-backed coplanar strip line, *IEEE Trans. Microwave Theory Tech.*, *45*, 87-94, 1997.

Yakovlev, A.B., and G.W. Hanson, Analysis of mode coupling on guided-wave structures using Morse critical points, *IEEE Trans. Microwave Theory Tech.*, in press, 1998.

Yamaguchi, S., A. Shimojima, and T. Hosono, Analysis of leaky modes supported by a slab waveguide,

Electron. Commun. Jpn., part 2, *73*(11), 20-31, 1990.

G. W. Hanson, Department of Electrical Engineering and Computer Science, University of Wisconsin-Milwaukee, 3200 North Cramer Street, Milwaukee, WI 53211. (e-mail: george@ee.uwm.edu)

A. B. Yakovlev, North Carolina State University, Center for Advanced Computing and Communication, Campus Box 7914, Raleigh, NC 27695-7914. (e-mail: yakovlev@eos.ncsu.edu)

(Received September 15, 1997; revised April 28, 1998; accepted April 30, 1998.)